


## ORIGINAL PAPER

# ACE2 and TMPRSS2 in human saliva can adsorb to the oral mucosal epithelium

Fucun Zhu<sup>1</sup> | Yi Zhong<sup>2,3</sup> | Huan Ji<sup>3,4</sup> | Ran Ge<sup>5</sup> | Lu Guo<sup>1</sup> | Haiyang Song<sup>2,3</sup> | Heming Wu<sup>3,4</sup> | Pengfei Jiao<sup>3,4</sup> | Sheng Li<sup>3,4</sup> | Chenxing Wang<sup>3,4</sup> | Hongming Du<sup>3,4</sup> 

<sup>1</sup>Department of Pathology, Fuzhou Children's Hospital of Fujian Province, Fuzhou, Fujian Province, P.R. China

<sup>2</sup>Department of General Dentistry, Affiliated Stomatological Hospital of Nanjing Medical University, Nanjing, Jiangsu Province, P.R. China

<sup>3</sup>Jiangsu Key Laboratory of Oral Disease, Nanjing Medical University, Nanjing, Jiangsu Province, P.R. China

<sup>4</sup>Department of Oral and Maxillofacial Surgery, Affiliated Stomatological Hospital of Nanjing Medical University, Nanjing, Jiangsu Province, P.R. China

<sup>5</sup>Department of Nuclear Medicine, Fujian Medical University Union Hospital, Fuzhou, Fujian Province, P.R. China

**Correspondence**

Hongming Du, MD, Ph.D., Department of Oral and Maxillofacial Surgery, Affiliated Stomatological Hospital of Nanjing Medical University, Hanzhong Road No.136, Nanjing, Jiangsu Province 210029, P.R. China.  
Email: dhm\_010@sina.com

**Funding information**

National Natural Science Foundation of China, Grant/Award Number: 81600908 and 81772887; Nature Science Foundation of Jiangsu Province, Grant/Award Number: BK2018040793; Health Committee of Jiangsu Province, Grant/Award Number: M2020003

**Abstract**

Severe acute respiratory syndrome coronavirus 2 (SARS-CoV-2) is primarily transmitted through droplets. All human tissues with the angiotensin-converting enzyme 2 (ACE2) and transmembrane protease serines 2 (TMPRSS2) are potential targets of SARS-CoV-2. The role of saliva in SARS-CoV-2 transmission remains obscure. In this study, we attempted to reveal ACE2 and TMPRSS2 protein expression in human parotid, submandibular, and sublingual glands (three major salivary glands). Then, the binding function of spike protein to ACE2 in three major salivary glands was detected. The expression of ACE2 and TMPRSS2 in human saliva from parotid glands were both examined. Exogenous recombinant ACE2 and TMPRSS2 anchoring and fusing to oral mucosal epithelial cells in vitro were also unraveled. ACE2 and TMPRSS2 were found mainly to be expressed in the cytomembrane and cytoplasm of epithelial cells in the serous acinus cells in parotid and submandibular glands. Our research also discovered that the spike protein of SARS-CoV-2 binds to ACE2 in salivary glands in vitro. Furthermore, exogenous ACE2 and TMPRSS2 can anchor and fuse to oral mucosa in vitro. Thus, the expression of ACE2 and TMPRSS2 in human saliva might have implications for SARS-CoV-2 infection.

**KEYWORDS**

ACE2, COVID-19, human salivary gland, oral mucosal epithelium, saliva, SARS-CoV-2, spike protein, TMPRSS2

Fucun Zhu, Yi Zhong, Huan Ji, and Ran Ge are equally contributed to this study.

This is an open access article under the terms of the Creative Commons Attribution-NonCommercial-NoDerivs License, which permits use and distribution in any medium, provided the original work is properly cited, the use is non-commercial and no modifications or adaptations are made.

© 2021 The Authors. *Journal of Anatomy* published by John Wiley & Sons Ltd on behalf of Anatomical Society

## 1 | INTRODUCTION

The SARS-CoV-2 has emerged as a global pandemic, causing a severe public health problem (Arshad et al., 2020). Like other human respiratory coronaviruses, such as severe acute respiratory syndrome coronavirus (SARS-CoV) and the middle east respiratory syndrome coronavirus, SARS-CoV-2 also belongs to genus- $\beta$  of the coronaviridae, involving multiple organs and tissues of the body (Cui et al., 2019; Hui et al. 2020).

The angiotensin-converting enzyme 2 (ACE2), known as a functional receptor for SARS-CoV, was first reported by Li (Li et al., 2003). Now, studies on SARS-CoV-2 have demonstrated that ACE2 also serves as the adsorption target for the SARS-CoV-2 spike protein 1 (Wan, et al., 2020). The SARS-CoV and the SARS-CoV-2 spike protein 1 can bind to ACE2 located on the host cytomembrane, facilitating the fusion and entry of the virus. This can culminate the adsorption and infection of the virus in the host cell (Xiao et al., 2003). The binding of the SARS-CoV-2 spike protein 1 to ACE2 protein of the host cell facilitates the entry of SARS-CoV-2 via TMPRSS2, a cytomembrane protease, and the deletion of TMPRSS2 can inhibit this process (Hoffmann et al., 2020). Thus, all human organs with ACE2 and TMPRSS2 are potential infectious targets of SARS-CoV-2 (Chai et al., 2020; Chen, Zhao, et al., 2020; Chen, Zhou, et al., 2020; Fan et al., 2020; Huang et al., 2020; Liu et al., 2020; Patel et al. 2020; Xu et al., 2020).

Respiratory droplets are the most common transmission route of SARS-CoV-2 (Singhal, 2020). It is reported that SARS-CoV-2 and SARS-CoV have been consistently detected in the infected patient's saliva (Azzi et al. 2020; To et al., 2020; Wang et al. 2004). The questionnaire for COVID-19 patients also indicated the functional abnormalities of salivary glands, such as hyposecretion (Chen, Zhao, et al., 2020; Chen, Zhou, et al., 2020). Based on the public database and bioinformatic analysis, some studies have reported the expression of ACE2 and TMPRSS2 in human salivary glands (Pascolo et al., 2020; Song et al., 2020; Shamsoddin, 2020; Wang et al., 2020). Only a couple of studies have demonstrated the presence of ACE2 in salivary glands just in the Chinese rhesus macaques and rats by histological method (Cano et al., 2019; Liu et al., 2011). However, the distribution details of the ACE2 and TMPRSS2 in human salivary glands and saliva remain unexplored.

In the current study, we have investigated ACE2 and TMPRSS2 distribution in major human salivary glands (parotid, submandibular, and sublingual glands) and the binding of ACE2 to the SARS-CoV-2 spike protein. We have also detected the expression of ACE2 and TMPRSS2 in human saliva and the anchoring and fusing function of exogenous ACE2 and TMPRSS2 to the oral mucosal epithelium *in vitro*. The current study aims to provide experimental evidence to expand the knowledge about the role of saliva in SARS-CoV-2 infection.

## 2 | MATERIALS AND METHODS

### 2.1 | Specimen acquisition

We procured parotid ( $n = 6$ ), submandibular ( $n = 6$ ), and sublingual ( $n = 7$ ) gland samples from adult patients afflicted with benign disorders of salivary glands. Samples were surgically resected in the

Affiliated Stomatological Hospital of Nanjing Medical University (Table 1). Saliva samples were collected from young healthy volunteers ( $n = 8$ ) parotid glands (Table 2) by a catheter inserted into the excretory duct via the parotid papilla to obtain saliva, avoiding the saliva pollution by other elements in the oral cavity. Specimens of the small intestine and prostate adenocarcinoma collected from Fuzhou Children's Hospital of Fujian Province and Fujian Provincial Hospital, respectively, served as the positive control for ACE2 and TMPRSS2 (Table 1). Specimens of adipose tissue and breast tissue collected from Fujian Provincial Hospital were used as the negative control for ACE2 and TMPRSS2 (Table 1). The current study was approved by the Medical Ethics Committee in Fuzhou Children's Hospital of Fujian Province. All patients signed the informed consent documents before the surgical procedure.

### 2.2 | ELISA to detect the binding of SARS-CoV-2 spike protein to ACE2 in human salivary glands

Salivary gland samples were homogenized on ice. The homogenate was crushed through the ultrasonication process. It was followed by centrifugation of homogenate at 5000 g for 5 min, and the supernatant was separated for further analysis. Protein estimation was done using Bicinchoninic Acid Kit (P0012, Beyotime, China). The SARS-CoV-2 spike protein (SARS-CoV-2 Spike S1-His Recombinant Protein, 40591-V08H3, Sino Biological, China) was diluted in PBS, and 1 ng/well was added into 96-well plates (Corning, USA) followed by overnight incubation at room temperature (RT). These plates were washed three times with Tween 20 solution with 0.05% TBS. Wells were blocked with 1% BSA in PBS for 1 h at RT. The supernatant of salivary gland homogenate was added to each well in triplicate and incubated overnight at RT. The plate was washed four times with PBS. ACE2 antibody (ACE2, 500 ng/ml, ab15348, Abcam, USA) was used to detect ACE2 receptor-bound spike proteins, followed by a thorough wash with Tween 20 with TBS-0.05%, three times, and 30 min incubation at RT with the HRP labeled Goat anti-rabbit IgG (1:2000, A0277, Beyotime, China). ABTS liquid substrate solution (Sigma, USA) was used for color development as per the manufacturer's instruction. OD (405 nm) was measured using an ELISA plate reader with wavelength correction set to 650 nm. HRP-labeled BSA (SE063, Solarbio, China) and HRP labeled goat anti-rabbit IgG served as control.

As the control for SARS-CoV-2 spike protein binding to ACE2 in human salivary glands, the homogenate of small intestine and breast tissue was used as the positive and negative control respectively.

### 2.3 | Western blotting for ACE2, TMPRSS2 and HIS tag detection

Western blot IP Kit (P0013, Beyotime, China) was used to extract the total protein from the salivary gland homogenate and cell lysates. Protein samples were separated by sodium dodecyl

TABLE 1 Patient demographics

Patient No.	Gender	Age(Year)	Location	Diagnosis
1	Female	56	Right parotid gland	Pleomorphic adenoma
2	Male	44	Left parotid gland	Pleomorphic adenoma
3	Male	51	Right parotid gland	Adenolymphoma
4	Male	28	Right parotid gland	Pleomorphic adenoma
5	Male	65	Right parotid gland	Adenolymphoma
6	Female	23	Right parotid gland	Sialolithiasis
7	Male	37	Left submandibular gland	Sialolithiasis
8	Male	35	Left submandibular gland	Sialolithiasis
9	Male	44	Left submandibular gland	Sialolithiasis
10	Female	32	Right submandibular gland	Sialolithiasis
11	Female	25	Left submandibular gland	Sialolithiasis
12	Male	31	Right submandibular gland	Sialolithiasis
13	Female	23	Right sublingual gland	Mucocele
14	Male	21	Right sublingual gland	Mucocele
15	Male	38	Left sublingual gland	Mucocele
16	Male	18	Right sublingual gland	Mucocele
17	Female	45	Right sublingual gland	Mucocele
18	Female	57	Right sublingual gland	Mucocele
19	Male	53	Left sublingual gland	Mucocele
20	Female	3	Small intestine	Intestinal obstruction
21	Male	0.8	Small intestine	Intussusception
22	Male	1	Small intestine	Intussusception
23	Female	0.3	Small intestine	Necrotizing enteritis
24	Male	5	Small intestine	Intestinal obstruction
25	Male	0.2	Small intestine	Megacolon
26	Male	73	Prostate	Prostate adenocarcinoma
27	Male	68	Prostate	Prostate adenocarcinoma
28	Male	70	Prostate	Prostate adenocarcinoma
29	Male	71	Prostate	Prostate adenocarcinoma
30	Male	73	Prostate	Prostate adenocarcinoma
31	Male	76	Prostate	Prostate adenocarcinoma
32	Female	63	Left Breast	Ductal carcinoma of breast
33	Female	52	Left Breast	Papillary carcinoma of breast
34	Female	73	Left Breast	Ductal carcinoma of breast
35	Female	34	Right Breast	Breast fibroma
36	Female	48	Right Breast	Papillary carcinoma of breast
37	Female	26	Left Breast	Breast fibroma
38	Female	3	Subcutaneous adipose	Intestinal obstruction

(Continues)

TABLE 1 (Continued)

Patient No.	Gender	Age(Year)	Location	Diagnosis
39	Male	0.2	Subcutaneous adipose	Megacolon
40	Male	68	Subcutaneous adipose	Prostate adenocarcinoma
41	Male	1	Subcutaneous adipose	Intussusception
42	Female	26	Subcutaneous adipose	Breast fibroma

TABLE 2 The demographics of saliva samples

Sample No.	Gender	Age(Year)	Collection site
1	Male	24	Left parotid gland
2	Male	24	Left parotid gland
3	Female	25	Left parotid gland
4	Male	25	Left parotid gland
5	Female	24	Left parotid gland
6	Female	24	Left parotid gland
7	Female	24	Left parotid gland
8	Male	26	Left parotid gland

sulfate-polyacrylamide gel electrophoresis and electroblotted to PVDF membranes (GE Healthcare Life Sciences, USA). Tris-buffer saline (TBS) containing 5% non-fat milk was used as the blocking agent. The primary antibodies (ACE2, 1 µg/ml, ab15348, Abcam, USA; TMPRSS2, 1:3000, ab109131, Abcam, USA; Anti-6X His tag antibody, 1:5000, ab213204, Abcam, USA; GAPDH, 1:1000, 5174, Cell Signaling Technology, USA) were added to the membranes and incubated at 4°C overnight and thoroughly washed with Tween 20 containing 0.05% TBS. It was followed by incubation with horseradish peroxidase-tagged secondary antibody (anti-rabbit IgG, 7074, Cell Signaling Technology, USA) for 1 h at RT. Blots were developed in the dark using ECL (Thermo Fisher Scientific, Germany) and visualized by exposure to enhanced chemiluminescence reagents (GE Healthcare, USA).

Previous studies have validated the distribution of the ACE2 in the small intestine (Hamming et al., 2004) and TMPRSS2 in prostate adenocarcinoma (Abcam, <https://www.abcam.cn/tmpRSS2-antibody-epr3862-ab109131.html>). There was no expression of ACE2 in breast tissue and TMPRSS2 in adipose tissue confirmed by the public database (<https://www.proteinatlas.org/>). The primary antibodies (ACE2 for small intestine and breast tissue, 1 µg/ml, ab15348, Abcam, USA; TMPRSS2 for prostate adenocarcinoma and adipose tissue, 1:3000, ab109131, Abcam, USA; anti-6x His tag antibody for HEK-293T transfected with a His-tagged Staphylococcus aureus cas9 and HEK-293T cells, 1:5000, ab213204, Abcam, USA; GAPDH, 1:1000, 5174, Cell Signaling Technology, USA) were used to detect target proteins. It was followed by incubation with HRP tagged secondary antibody (anti-rabbit IgG, 7074, Cell Signaling Technology, USA). The control without primary antibody was only incubated with HRP tagged secondary antibody (anti-rabbit IgG, 7074, Cell Signaling Technology, USA).

## 2.4 | IHC for ACE2 and TMPRSS2 detection in salivary glands

The dewaxed tissue sections were incubated with a drop of 3% H<sub>2</sub>O<sub>2</sub> at room temperature for 10 min to block endogenous peroxidase activity and later washed with PBS three times. The primary antibody ACE2 (2 µg/ml, ab15348, Abcam, USA) and TMPRSS2 (1:2000, ab109131, Abcam, USA) were added to each slide and incubated at RT for 2 h. After incubation, these slides were washed three times with PBS solution and incubated with the secondary antibody HRP-labeled anti-mouse/rabbit polymer (GK800511-B, Genetech, China) at RT for 30 min and re-washed three times with PBS solution. Subsequently, the diaminobenzidine (DAB) solution (Genetech, China) was added to each slide and incubated for 5 min. The tissue sections were counterstained with hematoxylin, dehydrated with alcohol gradient, renders tissues transparent with xylene, and fixed with neutral gum. ACE2 and TMPRSS2 immunoreactivity was grouped by immunoreactive score (IRS) (namely immunointensity score (IS) and proportion score (PS)) selected by staining intensity and distribution respectively. IS was divided into negative (0), weak (1), moderate (2), or strong (3), whereas PS was segmented into negative (<25% of the cells were immunoreactive) and positive (>25% of the cells were immunoreactive). Histological tissues were evaluated by two pathologists, respectively.

The positive and negative control tissue sections were stained using primary antibodies (ACE2 for small intestine and breast tissue, 2 µg/ml, ab15348, Abcam, USA; TMPRSS2 for prostate adenocarcinoma and adipose tissue, 1:2000, ab109131, Abcam, USA) and secondary antibody (HRP-labeled anti-mouse/rabbit antibody) respectively. The control without primary antibody was stained using HRP-labeled anti-mouse/rabbit antibody. The isotype control was stained using normal rabbit IgG (700 ng/ml, A7016, Beyotime, China) and HRP-labeled anti-mouse/rabbit antibody.

## 2.5 | ELISA for detecting ACE2 and TMPRSS2 in saliva from human parotid glands

Saliva samples were centrifugated at 2000 g for 10 min, and the supernatant was separated for further analysis. The Human Angiotensin-Converting Enzyme 2 ELISA Kit (CSB-E04489h, CUSABIO, China) was used to detect the ACE2 levels in saliva as per the manufacture's instruction. The TMPRSS2 expression in saliva was detected through the ELISA kit for Transmembrane Protease,

Serine 2 (SEC795Hu, Cloud-Clone Corp, USA) according to the instruction manufacture's instruction. OD (405 nm) was measured using the ELISA plate reader.

As the control for the expression of ACE2 in saliva, the homogenate of small intestine and breast tissue was used as the positive and negative control respectively. As the control for the expression of TMPRSS2 in saliva, the homogenate of prostate adenocarcinoma and adipose tissue were used as the positive and negative control respectively.

## 2.6 | ICC for exogenous ACE2 and TMPRSS2 detection in oral mucosa epithelial cells

Both human immortalized oral epithelial cells (HOEC, ATCC, USA) and human oral keratinocytes (HOK, Sciencell Research Laboratory, USA) were mature normal oral mucosa epithelial cell lines originating from human oral epithelium. They were cultured in Dulbecco's modified eagle medium (DMEM, Gibco, USA) with 10% fetal bovine serum (FBS, Gibco, USA) for 24h in a 6-well plate respectively. Before incubating exogenous ACE2 and TMPRSS2, each well was washed by PBS three times.

The Recombinant Human ACE2 with N-terminal His-Tag (JN0552, Biorab, China) and Recombinant TMPRSS2 with N-terminal His-Tag (375607, USBiological, USA) were diluted by PBS to the concentration of 0.38 ng/ml and 0.76 ng/ml (the concentration of ACE2 and TMPRSS2 in saliva) respectively. The diluted exogenous ACE2 and TMPRSS2 were added to HOEC and HOK cells (2.5 ml per well), respectively, and incubated at 37°C for 30 min. After that, the cells were washed by PBS three times and fixed with 4% paraformaldehyde. 0.3% Triton X-100 and BSA were used to penetrate the cytomembrane and block them. Primary antibody, namely Anti-6x His tag antibody (1:16000, ab213204, Abcam, USA), was added to each glass cover and incubated at RT for 2 h. After incubation, samples were washed three times with PBS solution and incubated with the secondary antibody Goat Anti-Rabbit IgG H&L (HRP) (1:9000, ab97051, Abcam, USA) at RT for 30 min and re-washed three times with PBS solution.

## 2.7 | Statistical analysis

All the statistical analysis was done using SPSS version 22.0 (IBM-Corp., USA). The difference between the three groups was analyzed by one-way analysis of variance. SNK-q test was used to make multiple comparisons.  $p < 0.05$  was considered to be statistically significant.

# 3 | RESULTS

## 3.1 | The expression of ACE2 and TMPRSS2 in salivary glands

Both ACE2 and TMPRSS2 were found to be expressed in salivary glands; however, their expression levels were significantly different among the three salivary glands. Lower than the ACE2 expression

of the parotid glands, the ACE2 in submandibular glands and sublingual glands were  $1.34 \pm 0.05$ -Fold (F) ( $p = 0.027$ ) and  $1.81 \pm 0.13$ -F ( $p = 0.003$ ) respectively (Figure 1a). Lower than the TMPRSS2 expression of the parotid glands, the TMPRSS2 in submandibular and sublingual glands were  $1.52 \pm 0.03$ -F ( $p = 0.001$ ) and  $4.85 \pm 0.02$ -F ( $p < 0.001$ ) respectively (Figure 1b).

The expression of ACE2 was positive in small intestine and negative in breast tissue (Figure 1d). The expression of TMPRSS2 was positive in prostate adenocarcinoma and negative in adipose tissue (Figure 1d). This result also confirmed the specificity of primary antibodies (ACE2 and TMPRSS2) used in this study. Salivary glands only stained by the secondary antibody were negative (Figure 1d).

## 3.2 | The spike protein of SARS-COV-2 absorbing to salivary glands

We observed that the spike protein of SARS-CoV-2 could bind to human salivary glands (parotid, submandibular, and sublingual glands). ELISA of salivary gland homogenate supernatant demonstrated that the ACE2 could bind to the spike protein of SARS-CoV-2 (Figure 2a-c).

As the control for the spike protein of SARS-CoV-2 binding to ACE2 in human salivary glands, the spike protein of SARS-CoV-2 was positively absorbed to the homogenate of small intestine and negatively absorbed to breast tissue (Figure 2d,e).

## 3.3 | The location of ACE2 and TMPRSS2 in salivary glands

The brownish-yellow ACE2 (Figure 3a) and TMPRSS2 (Figure 3b) immune-complex were observed in the cytoplasm and cytomembrane of epithelial cells from serous acinus, intercalated, secretory, and excretory ducts. The vascular endothelial cells were positively immunostained for the ACE2 immune complex (Figure 3a). ACE2 and TMPRSS2 complex staining was scored as 3 in parotid glands.

The mucinous acinar cells were found to be negatively immunostained for the brownish-yellow ACE2 (Figure 3c) and TMPRSS2 (Figure 3d) immune complex in submandibular glands. However, the immune complex of ACE2 and TMPRSS2 was observed in the cytoplasm and cytomembrane of serous acinar cells in the mixed acinus. The vascular endothelial cells were positively immunostained for the ACE2 immune complex (Figure 3c). ACE2 and TMPRSS2 complex staining was scored as 2 in submandibular glands.

The mucous acinar cells were found to be negatively immunostained for the brownish-yellow ACE2 (Figure 3e) and TMPRSS2 (Figure 3f) immune complex in sublingual glands. However, the ACE2 and TMPRSS2 immune complex was observed in the cytoplasm and cytomembrane of serous acinar cells in the mixed acinus. The vascular endothelial cells were positively immunostained for the ACE2 immune complex (Figure 3e). ACE2 and TMPRSS2 complex staining was scored as 1 in sublingual glands.

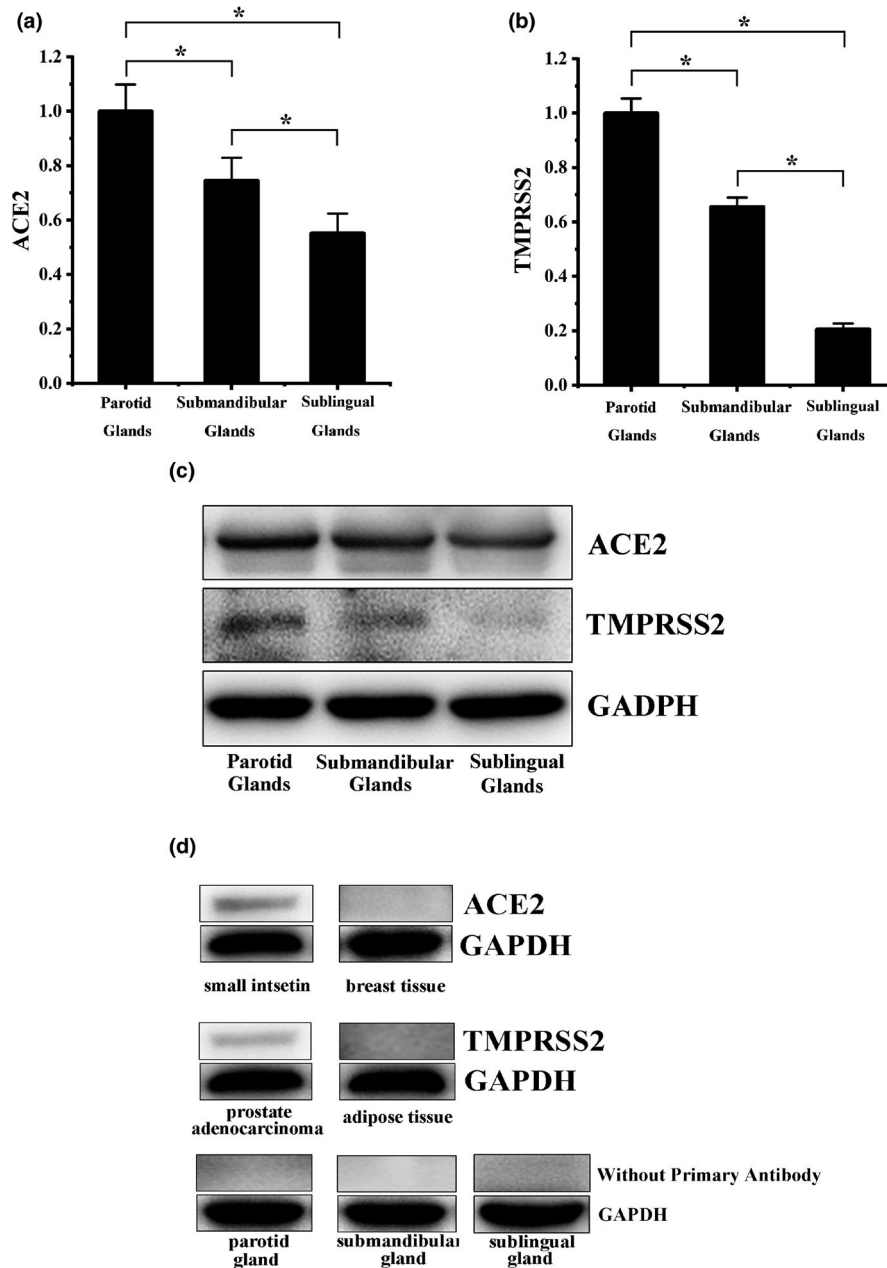


**FIGURE 1** The ACE2 and TMPRSS2 expression in salivary glands. (a) The ACE2 expression levels in parotid glands, submandibular glands, and sublingual glands, in descending order. (b) The TMPRSS2 expression levels in parotid glands, submandibular glands, and sublingual glands, in descending order. (c) The blots of ACE2 and TMPRSS2. (d) The controls in western blot. ACE2 was positive in small intestine and negative in breast tissue; TMPRSS2 was positive in prostate adenocarcinoma and negative in adipose tissue; and salivary glands only stained by the secondary antibody were negative

Intestinal villi were observed in the mucosal layer of the small intestinal epithelium (Figure 4a). The brownish-yellow ACE2 immune complex was observed in the small intestinal epithelium, which was used as the positive control for ACE2 immunostaining (Figure 4b). Normal breast tissue with luminal cells was surrounded by a basal layer of myoepithelial cells by HE staining (Figure 4c). There was no brownish-yellow ACE2 immune complex observed in breast tissue (Figure 4d). Adenocarcinoma of the prostate (Gleason grade  $3 + 4 =$  score of 7) presented with single, separate, well-formed glands in the prostate (Figure 4e). Prostate adenocarcinoma was

positive for the brownish-yellow TMPRSS2 immune complex, as the positive control for TMPRSS2 immunostaining (Figure 4f). H&E staining of mature adipocytes is presented in Figure 4g. There was no brownish-yellow TMPRSS2 immune complex observed in adipose tissue (Figure 4h). The parotid, submandibular and sublingual glands, only incubated with HRP-labeled anti-mouse/rabbit antibody, were found to be negative for immunostaining (Figure 4i). The parotid, submandibular, and sublingual glands, which were incubated with normal IgG and HRP-labeled anti-mouse/rabbit antibody, were also found to be negative for immunostaining (Figure 4j).



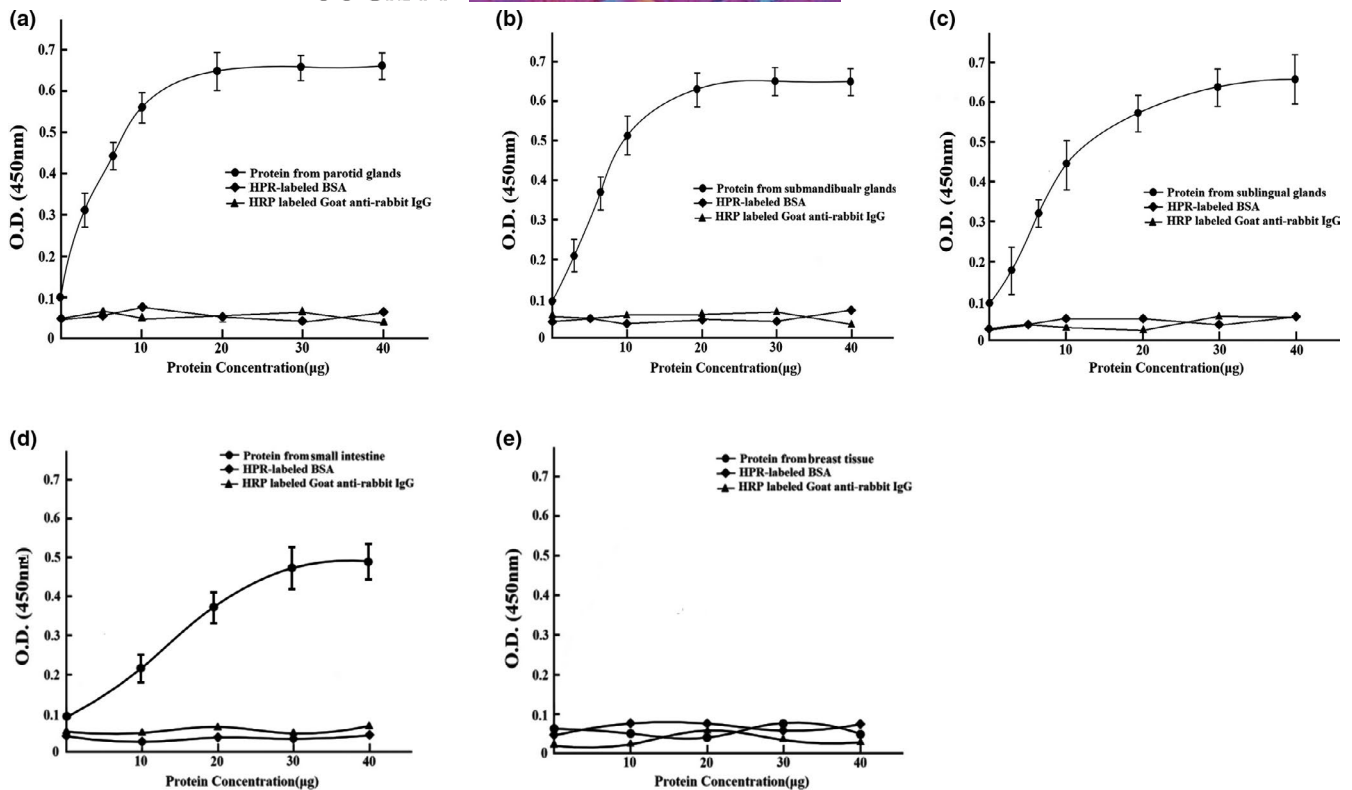


**FIGURE 2** The binding of SARS-CoV-2 spike protein with ACE2 in human salivary glands demonstrated by the ELISA. (a) The binding of SARS-CoV-2 spike protein with ACE2 in parotid glands. (b) The binding of SARS-CoV-2 spike protein with ACE2 in submandibular glands. (c) The binding of SARS-CoV-2 spike protein with ACE2 in sublingual glands. (d) The spike protein of SARS-CoV-2 was positively absorbed to the homogenate of small intestine. (e) The spike protein of SARS-CoV-2 was negatively absorbed to the homogenate of breast tissue

### 3.4 | The expression of ACE2 and TMPRSS2 in saliva from human parotid glands

The outcomes of ELISA showed that the concentration of ACE2 and TMPRSS2 in saliva was  $0.38 \pm 0.03$  ng/ml and  $0.76 \pm 0.18$  ng/ml respectively. As the control, the expression of ACE2 was positive in the homogenate of small intestine ( $0.91 \pm 0.12$  ng/ml) and negative in the homogenate of breast tissue ( $0.11 \pm 0.04$  ng/ml); the expression of TMPRSS2 was positive in the homogenate of prostate adenocarcinoma ( $0.87 \pm 0.10$  ng/ml) and negative in the homogenate of adipose tissue ( $0.05 \pm 0.03$  ng/ml).

### 3.5 | The exogenous ACE2 and TMPRSS2 absorbing to oral mucosa epithelial cells

The exogenous ACE2 and TMPRSS2 were found to exist in HOEC and HOK cells after incubating with recombinant human ACE2 and TMPRSS2 with His-tag. However, their expression levels were not significantly different between HOEC and HOK cells (Figure 5a,b). This result also confirmed the specificity of primary antibodies (His-tag) used in this study.

As the positive control, the expression of His-tag was positive in HEK-293T transfected with a His-tagged *Staphylococcus aureus* cas9 and negative in HEK-293T (Figure 5c). In the control

without primary antibodies, all results of samples were negative (Figure 5c).

Both HOEC and HOK cells were found to be positively immunostained for the brownish-yellow ACE2-anti His-tag (Figure 5d) and TMPRSS2-anti His-tag (Figure 5e) immune complex. The ACE2-anti His-tag and TMPRSS2-anti His-tag immune complex were observed in the cytomembrane of HOEC and HOK cells.

The brownish-yellow His-tag immune complex was observed in HEK-293T transfected with a His tagged *Staphylococcus aureus* cas9, which was used as the positive control for His-tag immunostaining (Figure 6a). There was no brownish-yellow His-tag immune complex observed in HEK-293T (Figure 6b). The HOEC and HOK, only stained by Goat Anti-Rabbit IgG H&L (HRP) antibody, were negative for immunostaining (Figure 6c). The HOEC and HOK incubated with normal IgG and Goat Anti-Rabbit IgG H&L (HRP) antibody were negatively immunostained (Figure 6d).

## 4 | DISCUSSION

A study in SARS-CoV infecting Chinese rhesus macaques has shown that the salivary glands of these animals possess ACE2, the function of which is affected by SARS-CoV infection (Liu et al., 2011). SARS-CoV-2 can use TMPRSS2 for spike protein priming. Thus camostat mesylate, an inhibitor of TMPRSS2, blocks the SARS-CoV-2 infection

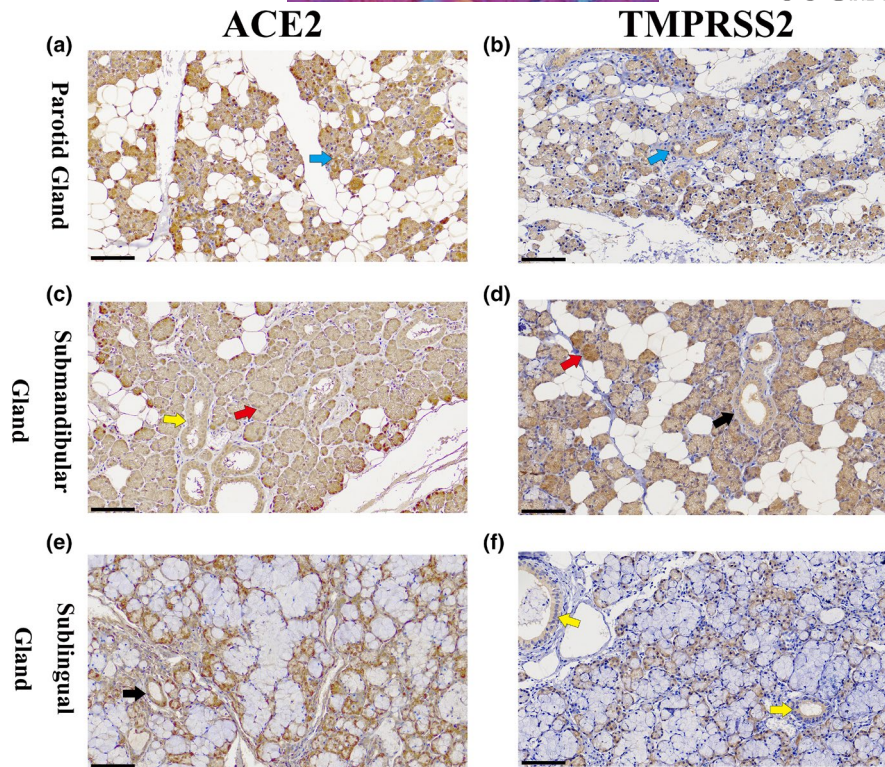


**FIGURE 3** IHC of salivary gland for the detection of ACE2 and TMPRSS2 complex. (a) IHC of parotid glands for the detection of ACE2. The brownish-yellow ACE2 immune complex was observed in the cytoplasm and cytomembrane of epithelial cells from serous acinar, sacral, secretory, excretory ducts, and vascular endothelial. (b) IHC of parotid glands for the detection of TMPRSS2 in parotid glands. The brownish-yellow TMPRSS2 immune complex was observed in the cytoplasm and cytomembrane of epithelial cells from serous acinar, sacral, secretory, excretory ducts, and vascular endothelial. (c) IHC of submandibular glands for the detection of ACE2. The brownish-yellow ACE2 immune-complex was mainly observed in the cytoplasm and cytomembrane of duct epithelial cells and serous acinus cells; the mucous acinar cells were negatively immunostained for the ACE2 immune complex. (d) IHC of submandibular glands for the detection of TMPRSS2. The brownish-yellow TMPRSS2 immune-complex was mainly observed in the cytoplasm and cytomembrane of duct epithelial cells and serous acinus cells; the mucous acinar cells were found to be negatively immunostained for the TMPRSS2 immune complex. (e) IHC of sublingual glands for the ACE2 detection. The mucous acinar cells were found to be negatively immunostained for the brownish-yellow ACE2 immune complex; the ACE2 immune complex was observed in the cytoplasm and cytomembrane of serous acinar cells in the mixed acinus. (f) IHC of sublingual glands for the detection of TMPRSS2. The mucous acinar cells were found to be negatively immunostained for the brownish-yellow TMPRSS2 immune complex, which was observed in the cytoplasm and cytomembrane of serous acinar cells in the mixed acinus (black scale bar = 100  $\mu$ m; black arrow: secretory duct; blue arrow: sacral ducts; yellow arrow: excretory ducts; red arrow: serous acinar cells) [Colour figure can be viewed at [wileyonlinelibrary.com](http://wileyonlinelibrary.com)]

of lung cells (Hoffmann et al., 2020). Chen et al. have reported xerostomia and parageusia in COVID-19 infected patients (Chen, Zhao, et al., 2020; Chen, Zhou, et al., 2020). There have been some studies confirming that ACE2 and TMPRSS2 are expressed in salivary glands. While the distribution details of the ACE2 and TMPRSS2 in human salivary glands still need to be explored (Pascolo et al., 2020; Song et al., 2020; Shamsoddin, 2020; Wang et al., 2020). This is the first study to demonstrate the expression and distribution details of the ACE2 and TMPRSS2 in the acinus and ducts cells of the human parotid, submandibular, and sublingual glands.

Mixed acini are composed of serous acinar cells and mucinous acinar cells. Parotid glands only contain serous acini, composed of serous acinar cells. Sublingual glands contain mixed acini mainly composed of mucous acinar cells. Submandibular glands contain mixed acini mainly composed of serous acinar cells (Delporte et al.,

**FIGURE 4** The controls for ACE2 and TMPRSS2 in IHC. (a) H and E staining of the small intestine. (b) The positive controls for ACE2: The brownish-yellow ACE2 immune complex was observed in the small intestinal epithelium. (c) H and E staining of the breast tissue. (d) The negative controls for ACE2: The brownish-yellow immune complex was not observed in the breast tissue. (e) H and E staining of prostate adenocarcinoma. (f) The positive controls for TMPRSS2: The brownish-yellow TMPRSS2 immune complex was observed in the prostate adenocarcinoma. (g) H and E staining of adipose tissue. (h) The negative controls for TMPRSS2: The brownish-yellow immune complex was not observed in the adipose tissue. (i) The controls without primary antibodies for ACE2 and TMPRSS2: The salivary glands were found to be negatively immunostaining. (j) The isotype controls for ACE2 and TMPRSS2 (normal rabbit IgG): The salivary glands were found to be negatively immunostaining. (black scale bar = 100  $\mu$ m) [Colour figure can be viewed at [wileyonlinelibrary.com](http://wileyonlinelibrary.com)]



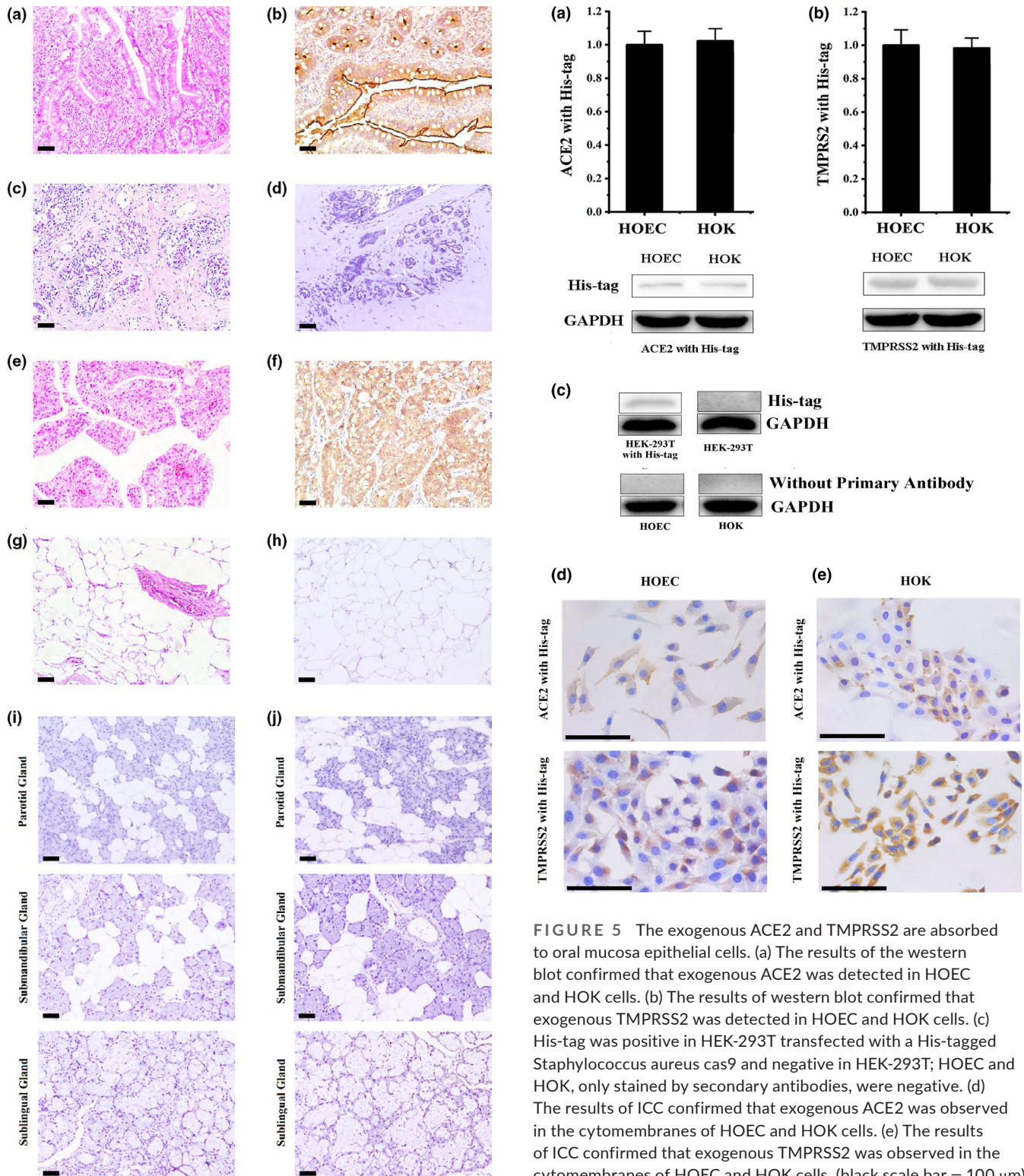


**FIGURE 5** The exogenous ACE2 and TMPRSS2 are absorbed to oral mucosa epithelial cells. (a) The results of the western blot confirmed that exogenous ACE2 was detected in HOEC and HOK cells. (b) The results of western blot confirmed that exogenous TMPRSS2 was detected in HOEC and HOK cells. (c) His-tag was positive in HEK-293T transfected with a His-tagged *Staphylococcus aureus* cas9 and negative in HEK-293T; HOEC and HOK, only stained by secondary antibodies, were negative. (d) The results of ICC confirmed that exogenous ACE2 was observed in the cytomembranes of HOEC and HOK cells. (e) The results of ICC confirmed that exogenous TMPRSS2 was observed in the cytomembranes of HOEC and HOK cells. (black scale bar = 100 μm) [Colour figure can be viewed at [wileyonlinelibrary.com](http://wileyonlinelibrary.com)]

2016). Our results indicated that ACE2 and TMPRSS2 were over-expressed in the cytoplasm of serous acinar cells in human salivary glands. Therefore, ACE2 and TMPRSS2 in saliva may be mainly secreted by the parotid and submandibular glands.

Respiratory droplets, originating from the nose, oral cavity, trachea, and lung, are one of the main transmission routes of SARS-CoV and SARS-CoV-2 (Ding et al., 2004; Vaz et al., 2020). Saliva is one of

the most important sources of droplets. SARS-CoV-2 is concentrated in the saliva of patients infected by COVID-19, which may come from the nose, mouth, trachea, and lung. Besides salivary glands, ACE2 expression has been validated in the nose, oral cavity, trachea, and lungs. The current study validated the positive expression of ACE2 and TMPRSS2 in saliva, indicating that saliva from parotid gland and

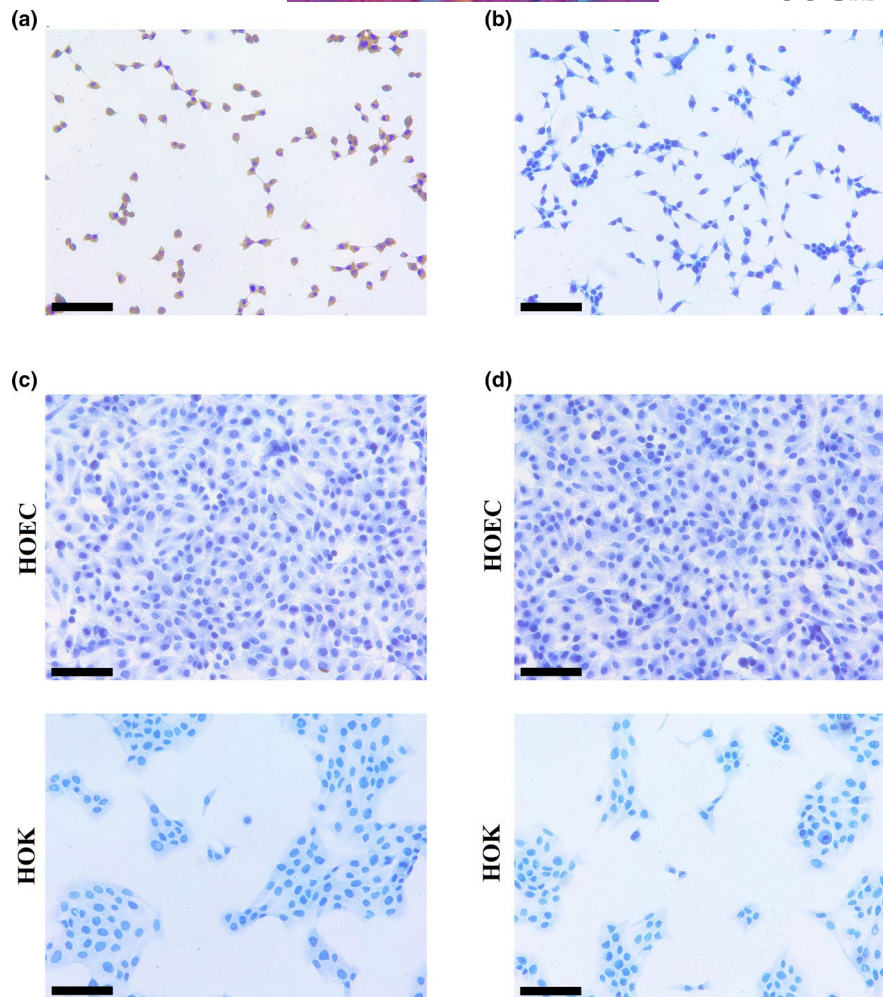


**FIGURE 6** The controls for His-tag in ICC. (a) The brownish-yellow His-tag immune complex was observed in HEK-293T transfected with a His-tagged *Staphylococcus aureus* cas9. (b) No immunostaining of His-tag was observed in HEK-293T. (c) The HOEC and HOK were negative for immunostaining stained by the secondary antibody. (d) The HOEC and HOK were negative for immunostaining stained by normal IgG and the secondary antibody. (black scale bar = 100  $\mu$ m) [Colour figure can be viewed at [wileyonlinelibrary.com](http://wileyonlinelibrary.com)]

submandibular gland may promote the infection of SARS-CoV-2. The spike protein of SARS-CoV and SARS-CoV-2 targeting ACE2 are highly similar in structure, and the fusion of both SARS-CoV and SARS-CoV-2 depends on TMPRSS2 (Bertram et al., 2012; Kuba et al., 2005; Li et al., 2003; Wan et al., 2020). Thus, saliva may promote the infection of SARS-CoV.

Our results confirmed that saliva contains ACE2 and TMPRSS2. The exogenous ACE2 and TMPRSS2 can absorb to oral mucosa epithelial cells. Based on results mentioned above, we hypothesized that the ACE2 and TMPRSS2 secreted into saliva from the cytoplasm of serous acinar cells in human salivary glands might anchor and fuse to oral mucosa epithelium, and perhaps they could contribute to SARS-CoV-2 infection in vivo. It is reported that live SARS-CoV-2 was detected in saliva. Moreover, saliva contains the three key elements (ACE2, TMPRSS2, and SARS-CoV-2) of SARS-CoV-2 infection (To et al., 2020). This is the first study demonstrating that ACE2 and TMPRSS2 are expressed in saliva and binds to oral mucosa epithelium. Therefore, saliva may be a promoter of SARS-CoV-2 infection.

Saliva is mainly composed of water and secreted by serous acinar cells, assisting in maintaining the moisture in the mouth, swallowing, and oral self-cleaning. In the resting state of saliva secretion, parotid glands account for 25%, and the submandibular glands account for 60%. However, in the highly stimulated state, parotid glands account for 50%, and the submandibular glands account for 35% of the total salivary secretion (Jensen et al., 1998). Some SARS-CoV-2 infected patients develop a dry mouth and abnormal taste. And some other cases present oral necrotic ulcers and aphthous-like ulcerations, which develop early in the course of disease after the development of dysgeusia and affect the function of the tongue, lips, palate, and oropharynx. (Brandão et al. 2021; Chen, Zhao, et al., 2020; Chen, Zhou, et al., 2020). It may be attributed to the SARS-CoV-2 infection of serous acinar cells in the parotid and submandibular glands and oral mucosa, which may cause salivary hyposalivation and inflammatory damage. In addition to the direct inflammatory reaction caused by SARS-CoV-2, other factors causing hyposalivation of saliva in COVID-19 infected patients include water-electrolyte imbalance and medication. As SARS-CoV-2 targets parotid and submandibular



glands, the SARS-CoV-2 infected patients may present the symptoms and signs of the parotid and submandibular glands sialadenitis, such as swelling, discomfort, and pain. These may be considered as early signs and symptoms of COVID-19 infection not reported in public. Thus, these need to receive more attention.

The findings of our study validated that the cytomembrane and cytoplasm of serous acinar epithelial cells in the parotid gland contain a high number of ACE2 and TMPRSS2 that facilitate the adsorption and fusion of SARS-CoV-2. We hypothesized that SARS-CoV-2 replicates in serous acinar cells and is released by cytolysis into the saliva. The previous study has reported the presence of SARS-CoV-2 nucleotides in the saliva of infected patients, and the viral culture of these saliva samples demonstrated the existence of the live virus in saliva (To et al., 2020). Moreover, salivary amylase might get released into the peripheral blood after cytolysis of SARS-CoV-2 infected serous acinar cells. Thus, there is a possibility that the peripheral blood of COVID-19 infected patients may demonstrate the presence of salivary amylase. This may act as a vital indicator of the parotid gland damage in SARS-CoV-2 infected patients.

The outcome of our investigation demonstrated that ACE2 and TMPRSS2 are distributed in the cytomembrane and cytoplasm of intercalated ducts, and the SARS-CoV-2 infection might cause a series of destructive inflammatory reactions. Previous studies have confirmed that intercalated duct epithelium possesses stem cell characteristics with the potential to get differentiated into acinar cells and secretory duct epithelium (Kwak et al., 2016; May et al., 2018; Ninche et al., 2020). The damage to the intercalated duct epithelium might affect the repair of the acinus and secretory ducts caused by inflammation.

## 5 | CONCLUSION

ACE2 and TMPRSS2 are expressed in the cytoplasm of serous acinar cells in human salivary glands. The exogenous ACE2 and TMPRSS2 can anchor and fuse to epithelial cells of the oral mucosa. ACE2 and TMPRSS2 are expressed in human saliva, suggesting susceptibility to SARS-CoV-2 infection.

## ACKNOWLEDGMENTS

This work was supported by the National Natural Science Foundation of China (No. 81600908 and 81772887), the Nature Science Foundation of Jiangsu Province (No. BK2018040793), the Health Committee of Jiangsu Province (No. M2020003). The authors declare no potential conflicts of interest with respect to the authorship and/or publication of this article.

## AUTHORS CONTRIBUTION

F Zhu, Y Zhong, H Ji, R Ge, H Du, contributed to conception and design; L Guo, H Song, H Wu, P Jiao, S Li, C Wang contributed to conception. F Zhu, Y Zhong, R Ge, H Ji, H Du, contributed to acquisition, analysis and interpretation; L Guo, H Song contributed

to acquisition and analysis; H Wu, P Jiao, S Li, C Wang contributed to interpretation. F Zhu, Y Zhong, H Ji, R Ge, H Du, drafted the manuscript. All authors revised the manuscript then gave final approval.

## DATA AVAILABILITY STATEMENT

The datasets generated and/or analyzed during the current study are not publicly available but are available from the corresponding author upon reasonable request.

## ORCID

Hongming Du  <https://orcid.org/0000-0002-0909-0773>

## REFERENCE

- Arshad Ali, S., Baloch, M., Ahmed, N., Arshad Ali, A. & Iqbal, A. (2020) The outbreak of coronavirus disease 2019 (COVID-19)-an emerging global health threat. *Journal of Infection and Public Health*, 13(4), 644–646. S1876-0341:0365-8.
- Azzi, L., Carcano, G., Gianfagna, F., Grossi, P., Gasperina, D.D., Genoni, A. et al. (2020) Saliva is a reliable tool to detect SARS-CoV-2. *Journal of Infection*, 81(1), e45–e50. pii: S0163-4453:0213-30219.
- Bertram, S., Heurich, A., Lavender, H., Gierer, S., Danisch, S., Perin, P. et al. (2012) Influenza and SARS-coronavirus activating proteases TMPRSS2 and HAT are expressed at multiple sites in human respiratory and gastrointestinal tracts. *PLoS One*, 7, e35876.
- Brandão, T.B., Gueiros, L.A., Melo, T.S., Prado-Ribeiro, A.C., Nesrallah, A.C., Prado, G.V. et al. (2021) Oral lesions in patients with SARS-CoV-2 infection: could the oral cavity be a target organ? *Oral Surg Oral Med Oral Pathol Oral Radiol*, 131, e45–e51.
- Cano, I.P., Dionisio, T.J., Cestari, T.M., Calvo, A.M., Colombini-Ishikiriana, B.L., Faria, F.A.C. et al. (2019) Losartan and isoproterenol promote alterations in the local renin-angiotensin system of rat salivary glands. *PLoS One*, 14, e0217030.
- Chai, X.Q., Hu, L.F., Zhang, Y., Han, W., Lu, Z., Ke, A. et al. (2020) Specific ACE2 expression in cholangiocytes may cause liver damage after 2019-nCoV infection. *bioRxiv*. p. 2020.02.03.931766.
- Chen, L.L., Zhao, J.J., Peng, J.F., Li, X., Deng, X., Geng, Z. et al. (2020) Detection of SARSCoV-2 in saliva and characterization of oral symptoms in COVID-19 patients. *Cell Proliferation*, 53, e12923. <http://dx.doi.org/10.1111/cpr.12923>
- Chen, N., Zhou, M., Dong, X., Qu, J., Gong, F., Han, Y. et al. (2020) Epidemiological and clinical characteristics of 99 cases of 2019 novel coronavirus pneumonia in Wuhan, China: a descriptive study. *Lancet*, 395, 507–513.
- Cui, J., Li, F., Shi, Z-L. (2019) Origin and evolution of pathogenic coronaviruses. *Nature Reviews Microbiology*, 17, 181–192. <http://dx.doi.org/10.1038/s41579-018-0118-9>
- Delporte, C., Bryla, A. & Perret, J. (2016) Aquaporins in salivary glands: from basic research to clinical applications. *International Journal of Molecular Sciences*, 17, 166.
- Ding, Y., He, L.I., Zhang, Q., Huang, Z., Che, X., Hou, J. et al. (2004) Organ distribution of severe acute respiratory syndrome (SARS) associated coronavirus (SARS-CoV) in SARS patients: implications for pathogenesis and virus transmission pathways. *The Journal of Pathology*, 203, 622–630.
- Fan, C.B., Li, K., Ding, Y.H., Lu, W.L. & Wang, J. (2020) ACE2 expression in kidney and testis may cause kidney and testis damage after 2019-nCoV infection. *MedRxiv*, 2020.02.12.20022418.
- Hamming, I., Timens, W., Bulthuis, M., Lely, A.T., Navis, G.J. & van Goor, H. (2004) Tissue distribution of ACE2 protein, the functional receptor for SARS coronavirus. A first step in understanding SARS pathogenesis. *The Journal of Pathology*, 203, 631–637.

- Hoffmann, M., Kleine-Weber, H., Schroeder, S., Krüger, N., Herrler, T., Erichsen, S. et al. (2020) SARS-CoV-2 cell entry depends on ACE2 and TMPRSS2 and is blocked by a clinically proven protease inhibitor. *Cell*, 181, 271–280.
- Huang, C., Wang, Y., Li, X., Ren, L., Zhao, J., Hu, Y.I. et al. (2020) Clinical features of patients infected with 2019 novel coronavirus in Wuhan, China. *Lancet*, 395, 497–506.
- Hui, D.S., I Azhar, E., Madani, T.A., Ntoumi, F., Kock, R., Dar, O. et al. (2020) The continuing 2019-nCoV epidemic threat of novel coronaviruses to global health—the latest 2019 novel coronavirus outbreak in Wuhan, China. *International Journal of Infectious Diseases*, 91, 264–266.
- Jensen, J.L., Karatsaidis, A. & Brodin, P. (1998) Salivary secretion: stimulatory effects of chewing-gum versus paraffin tablets. *European Journal of Oral Sciences*, 106, 892–896.
- Kuba, K., Imai, Y., Rao, S., Gao, H., Guo, F., Guan, B. et al. (2005) A crucial role of angiotensin converting enzyme 2 (ACE2) in SARS coronavirus-induced lung injury. *Nature Medicine*, 11, 875–879.
- Kwak, M., Alston, N. & Ghazizadeh, S. (2016) Identification of stem cells in the secretory complex of salivary glands. *Journal of Dental Research*, 95, 776–783.
- Li, W., Moore, M.J., Vasilieva, N., Sui, J., Wong, S.K., Berne, M.A. et al. (2003) Angiotensin-converting enzyme 2 is a functional receptor for the SARS coronavirus. *Nature*, 426, 450–454.
- Liu, L., Wei, Q., Alvarez, X., Wang, H., Du, Y., Zhu, H. et al. (2011) Epithelial cells lining salivary gland ducts are early target cells of severe acute respiratory syndrome coronavirus infection in the upper respiratory tracts of rhesus macaques. *Journal of Virology*, 85, 4025–4030.
- Liu, Y., Yang, Y., Zhang, C., Huang, F., Wang, F., Yuan, J. et al. (2020) Clinical and biochemical indexes from 2019-nCoV infected patients linked to viral loads and lung injury. *Science China Life Sciences*, 63, 364–374.
- May, A.J., Cruz-Pacheco, N., Emmerson, E., Gaylord, E.A., Seidel, K., Nathan, S. et al. (2018) Diverse progenitor cells preserve salivary gland ductal architecture after radiation-induced damage. *Development*, 145:dev166363.
- Ninche, N., Kwak, M. & Ghazizadeh, S. (2020) Diverse epithelial cell populations contribute to the regeneration of secretory units in injured salivary glands. *Development*, 147(19):dev192807.
- Pascolo, L., Zupin, L., Melato, M., Tricarico, P.M. & Crovella, S. (2020) TMPRSS2 and ACE2 coexpression in SARS-CoV-2 salivary glands infection. *Journal of Dental Research*. 22034520933589.
- Patel, A., Jernigan, D.B., Abdirizak, F., Abedi, G., Aggarwal, S., Albina, D. et al. (2020) Initial public health response and interim clinical guidance for the 2019 novel coronavirus outbreak – United States, December 31, 2019–February 4, 2020. *American Journal of Transplantation*, 20(3):889–895. <http://dx.doi.org/10.1111/ajt.15805>
- Shamsoddin, E. (2020) Saliva: a diagnostic option and a transmission route for 2019-nCoV. *Evidence-Based Dentistry*, 21, 68–70.
- Singhal, T. (2020) A review of coronavirus disease-2019 (COVID-19). *Indian Journal of Pediatrics*, 87, 281–286.
- Song, J., Li, Y., Huang, X., Chen, Z., Li, Y., Liu, C. et al. (2020) Systematic analysis of ACE2 and TMPRSS2 expression in salivary glands reveals underlying transmission mechanism caused by SARS-CoV-2. *Journal of Medical Virology*, 92(11):2556–2566. <https://doi.org/10.1002/jmv.26045>
- To, K.K., Tsang, O.T., Chik-Yan Yip, C., Chan, K.H., Wu, T.C., Chan, J.M. et al. (2020) Consistent detection of 2019 novel coronavirus in saliva. *Clinical Infectious Diseases*. pii:ciaa149.
- Vaz, S.N., deSantana, D.S., Netto, E.M., Pedrosa, C., Wang, W.-K., Santos, F.D.A., et al. (2020) Saliva is a reliable, non-invasive specimen for SARS-CoV-2 detection. *The Brazilian Journal of Infectious Diseases*, 24(5), 422–427. <http://dx.doi.org/10.1016/j.bjid.2020.08.001>
- Wan, Y., Shang, J., Graham, R., Baric, R.S. & Li, F. (2020) Receptor recognition by novel coronavirus from Wuhan: an analysis based on decade-long structural studies of SARS. *Journal of Virology*, 94, pii: e00127–20.
- Wang, C., Wu, H., Ding, X.U., Ji, H., Jiao, P., Song, H. et al. (2020) Does infection of 2019 novel coronavirus cause acute and/or chronic sialadenitis? *Medical Hypotheses*, 140, 109789.
- Wang, W.-K., Chen, S.-Y., Liu, I.-J., Chen, Y.-C., Chen, H.-L., Yang, C.-F. et al. (2004) Detection of SARS-associated coronavirus in throat wash and saliva in early diagnosis. *Emerging Infectious Diseases*, 10, 1213–1219.
- Xiao, X., Chakraborti, S., Dimitrov, A.S., Gramatikoff, K. & Dimitrov, D.S. (2003) The SARS-CoV S glycoprotein: expression and functional characterization. *Biochemical and Biophysical Research Communications*, 312, 1159–1164.
- Xu, H., Zhong, L., Deng, J., Peng, J., Dan, H., Zeng, X. et al. (2020) High expression of ACE2 receptor of 2019-nCoV on the epithelial cells of oral mucosa. *International Journal of Oral Science*, 12, 8.

**How to cite this article:** Zhu, F., Zhong, Y., Ji, H., Ge, R., Guo, L., Song, H., et al (2022) ACE2 and TMPRSS2 in human saliva can adsorb to the oral mucosal epithelium. *Journal of Anatomy*, 240, 398–409. <https://doi.org/10.1111/joa.13560>